

3-Dimensional Visual Navigation for Repetitive Transcranial Magnetic Stimulation Treatment

‡Yoshihiro Yasumuro*
Faculty of Environmental
and Urban Engineering,
Kansai University

‡Masaki Sekino
Dept. of Electrical
Engineering and
Information Systems,
Grad School of Engineering,
The University of Tokyo

Tatsuya Ogino
Faculty of Environmental
and Urban Engineering,
Kansai University

‡Taiga Matsuzaki
Home Healthcare Research
& Development Department,
Teijin Pharma Limited

Masahiko Fuyuki
Faculty of Environmental
and Urban Engineering,
Kansai University

Kouichi Hosomi
Dept. of Neuromodulation
and Nuerosurgery,
Osaka University‡

‡Atsushi Nishikawa
Faculty of Textile Science
and Technology,
Shinshu University

Youichi Saitoh
Dept. of Neuromodulation
and Nuerosurgery,
Osaka University‡

ABSTRACT

Repetitive transcranial magnetic stimulation (rTMS) is a non-invasive method for treating various neurological and psychiatric disorders. This paper focuses on a treatment for neuropathic pain that can be caused by a lesion or disease of the central or peripheral nervous system, including stroke, trauma or surgical operation. With the growing demands of neuropathic pain patients and their increasing numbers, rTMS treatment tools are becoming more necessary. rTMS uses electromagnetic induction to induce weak electric currents by rapidly changing the magnetic field. Targeting a specific part of the brain to locate the magnetic field works as a treatment for pain relief. However, the current style of rTMS treatment is still developing and is so technically specialized that only a limited number of hospitals and only a handful of specialists can provide this therapy. The existing systems of rTMS are based on an optical marker-based 3-dimensional (3D) sensing technique for positioning the stimulation coil to target the small spot in the region of interest in the brain, and for referring pre-scanned MRI data to check the target position. Furthermore, this system requires the patient to be fixed on a bed in which optical markers for 3D sensing are placed during the treatment to maintain positioning precision. We propose a constraints-free style of the rTMS system, which employs a markerless method for positioning the patient's head with imaging sensors. Utilizing the patient's face shape instead of the positioning markers, this paper shows the potential for achieving a relaxed curative environment and an easy-to-handle system framework.

Index Terms: H.5.2 [INFORMATION INTERFACES AND PRESENTATION]: User Interfaces—Graphical user interfaces (GUI); I.4.8 [IMAGE PROCESSING AND COMPUTER VISION]: Scene Analysis—Tracking; J.3 [LIFE AND MEDICAL SCIENCES]: Medical information systems—

1 INTRODUCTION

Repetitive transcranial magnetic stimulation (rTMS) has been gathering attention as a non-invasive method for treating various neurological and psychiatric disorders including strokes, Parkinson's disease, and depression. This paper focuses on a new treatment to alleviate neuropathic pain that can be caused by a lesion or disease of the central or peripheral nervous system, including stroke, trauma or surgical operation. rTMS uses electromagnetic induction to induce weak electric currents by rapid change of a pulsed magnetic field; thus, rTMS treatment is capable of stimulating specific parts

* e-mail: yasumuro@kansai-u.ac.jp

of the brain, the primary motor area for the neuropathic pains for instance, with minimal discomfort in a non-invasive manner [5, 3].

The existing treatment method of rTMS is achieved by an optical 3-dimensional (3D) sensing technique for positioning the stimulation coil to target the spot in the brain that needs to be cured [12, 10, 8]. As shown in the Figure 1, before the treatment, the doctors are supposed to measure the 3D position of the feature points on the patients head; the nasal point, nose top and anterior auricular points, for instance. These positions allow the system to register the MRI data of the preoperative examination in the sensor coordinate by using the corresponding feature points in the MRI data. Then the positioning sensor tracks the coil, using a set of optical markers installed on it. Showing the relative position of the coil and the registered MRI data helps the doctor to target the spot in the brain. To ensure the positioning accuracy during the treatment, the patient must be immobilized on the bed throughout the treatment, because the registered patient's feature points are based on the optical markers fixed on the bed.

On the other hand, since the effects of rTMS last only several hours, rTMS treatments need to be available whenever the patient needs these treatments. In fact, rTMS treatments are only available at specialized clinics such as university hospitals, because only experienced physicians in a limited number of hospitals can use the expensive and complicated rTMS system in its present circumstances. Fukushima et al. proposed a magnetic navigation system designed for home use of rTMS [2], using inexpensive and small magnetic sensors. By collecting the spatial data samples of the magnetic field to record the proper position and orientation of the stimulation coil at the initial treatment by an expert doctor, the system can help the user navigate and reproduce the coil position to target the treatment spot for subsequent treatments at home. This system theoretically allows any users, even those without medical knowledge and techniques to easily locate the coil for subsequent treatment. The magnetic sensors are fixed on a glasses-style mount device which the user can easily wear when applying the treatment



Figure 1: Current rTMS Procedure Example

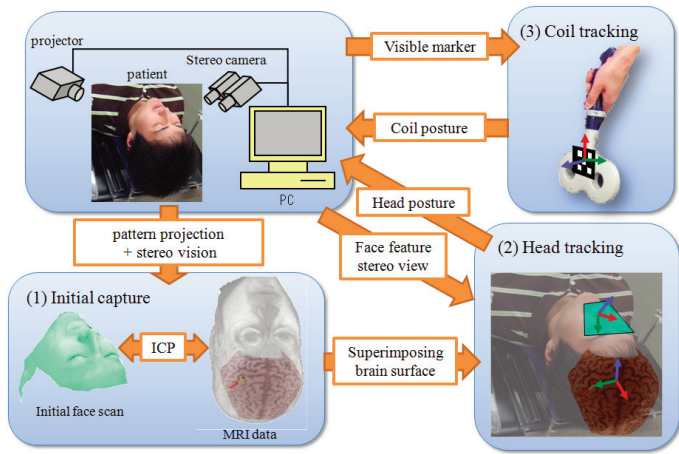


Figure 2: Proposed System Process

with no need to be constrained on the bed. Since the positioning accuracy depends on the reproducibility of wearing the glasses-style mount device, that device must be elaborately designed for adjustment to the individual patient in practical steps.

This paper proposes a new system framework that achieves both a constraints-free manner for patient use and stable positioning accuracy independent of the sensor mounting conditions.

2 APPROACH

Our system utilizes image sensing for non-contact 3D positioning, employing a stereo-video camera. The basic idea is to use a set of visible features of the patient's face as a tracking target so the positioning system is independent from both the marker setup and the sensor mount on the patient. Figure 2 shows an overview of the proposed system. The principal components are initial alignment, head-tracking and coil-tracking functionalities.

Initial alignment procedure fits the MRI volume data to the user's face surface shape so that the brain geometry in the MRI volume is properly located to the live position of the user's head. The human face has many smooth areas without clear image features such as the cheeks and forehead. Passive measurement of the stereo camera may produce sparse shape data from such area. To acquire dense shape data for a stable fitting, we project a random pattern of dots from a projector onto the users face while the stereo camera captures the initial face shape. This shape-fitting procedure is done by an iterative computation to find a transform that gives the best match of the two-shape data sets, and the successive head motion is a relative transform of this initial head alignment.

The head tracking requires a realtime rate process for monitoring the live head motion of the patient without using physical constraints, assuming that the patient may sit at the doctor for face-to-face communication for instance, during the treatment. To achieve realtime head tracking, we apply the image feature tracking to give the corresponding points between the consecutive stereo camera frames over time. Each image feature, including eye corners, nose top, and corners of the mouth are tracked on both cameras, and their 3D coordinates are computed. Assuming that the set of face features has no deformation, a 3D transform to give the best match between the two face feature sets is found. Because the camera frame interval is short enough to capture a sitting patient, the displacements between the frames are not so large. Therefore, the iteration of this computation can reach convergence in a limited time.

For the coil tracking, we use a marker-based method, since installing and permanently maintaining the markers on the coil is allowed. Visible features of the markers can be registered and tracked

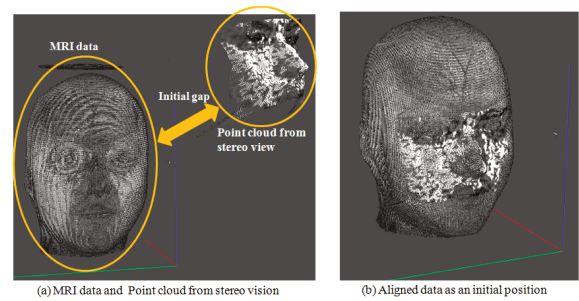


Figure 3: Initial Alignment

for their positioning by the identical stereo camera, and thus the MRI data, the patient head and the coil geometries are integrated in the same camera coordinate. Relative positions and the orientations can be monitored and used for navigating the coil to the target spot on the brain.

3 INITIAL ALIGNMENT

For the initial alignment, the surface of the MRI is prepared by extracting the boundary surface dots between the areas of the air and the human skin in the MRI volume preliminarily. Using a random pattern projection to provide visible features on the patient's face surface, the stereo camera is capable of capturing the face shape as a set of dense points. Both the surface shape of the MRI and the patient's face are unorganized 3D point sets. To fit these point sets, we use the ICP (iterative closest point)[1].

The ICP is an iterative algorithm often employed to find a rigid-body motion by minimizing the difference between two shape data sets of point clouds a and b as shown in equation(1). Since the human face shape has a certain variation around eyes, nose, and mouth, the ICP is expected to be applicable for searching the proper corresponding points to fit together between the point sets.

$$E = \sum_{i=1}^N (Ra_i + t - b_i)^T (Ra_i + t - b_i) \quad (1)$$

The inputs are the two point sets from the MRI and the stereo camera. The initial estimation of the transformation to fit the MRI data to the stereo camera data is the output, which is a refined result of transformation with rotation R and translation t to fit them together as in the following steps:

1. Associate points by the nearest neighbor criteria.
2. Estimate transformation parameters using a mean square cost function (1).
3. Transform the points using the estimated parameters.
4. Re-associate the points and iterate.

4 HEAD TRACKING

Initial alignment gives the 3D geometrical relation between the live face and the brain in the MRI. Transformation between the initial and current faces virtually superimposes the MRI brain onto the current physical brain in the live patient's head. Our head tracking to find the 3D transform of the face data is based on Matsumoto's method [9]. We selected the corners of the eyes, nose, head, and corners of the mouth as clear image features in the patient's face instead of putting in artificial markers. The criterion of the difference Equation (2)) to be minimized is similar to that of ICP, but computation is much simpler, since the corresponding pairs of the points are known and the number of points is small.

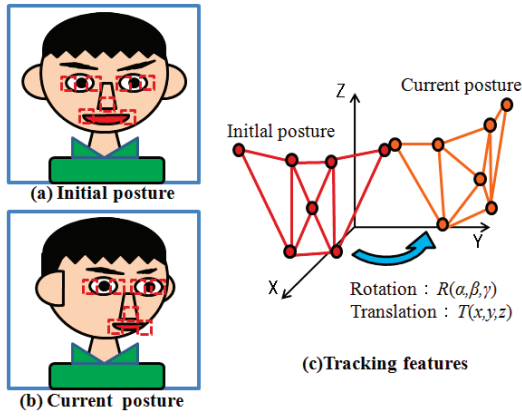


Figure 4: Head Tracking based on Face Features

$$J = \sum_{i=1}^M w_i (Rx_i + t - y_i)^T (Rx_i + t - y_i), \quad (2)$$

where, N is the number of the tracking points ($N = 7$ in this paper), x_i is the initial 3D coordinates for the feature i , y_i is the current 3D coordinate for the feature and w_i is the weight factor for each corresponding pair. The searching process for finding corresponding points of the 7-face features is based on template matching, in which a small image region is defined as a template for each feature point in the initially captured frame. We use normalized correlation coefficient (NCC) for the matching criterion and the weight factor of w_i as in Matsumoto's method. NCC works as a reliability of the corresponding points and thus the higher w_i gives higher priority to the more reliable corresponding features.

$$w_i = \frac{\sum_{v=1}^M \sum_{u=1}^N \phi(u, v) \varphi(u, v)}{\sqrt{\sum_{v=1}^M \sum_{u=1}^N \phi(u, v)^2 \sum_{v=1}^M \sum_{u=1}^N \varphi(u, v)^2}}, \quad (3)$$

$$\phi(u, v) = I(u, v) - \frac{\sum_{v=1}^M \sum_{u=1}^N I(u, v)}{NM} \quad (4)$$

$$\varphi(u, v) = T_i(u, v) - \frac{\sum_{v=1}^M \sum_{u=1}^N T_i(u, v)}{NM} \quad (5)$$

where, the current frame image is I , the template image is T_i (size: $M \times N$).

For effectively narrowing the feature searching area, we apply face-tracking on the frame before the template matching. We use a combination of a Haar-Like feature [7] and an Adaboost training algorithm [14] implemented in OpenCV library [15].

5 COIL TRACKING

Since the stimulation coil is specialized for medical use, the coil can be maintained with a specific marker installed for the curing process (Figure 5). Detecting the marker from both images of the captured frame pair by the stereo camera, corner points of the marker can be easily specified and triangulated for acquiring a 3D coordinate to monitor the coil position and orientation. Image processing for the marker detection is as follows (see also Figure 6):

1. Make binary images from the captured frames.
2. Labeling the dark closed areas.
3. Select rectangles by counting the corners for each closed area.

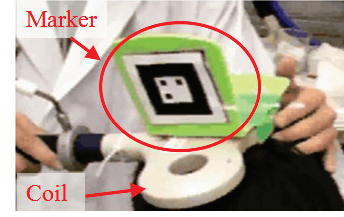


Figure 5: Coil with a Marker

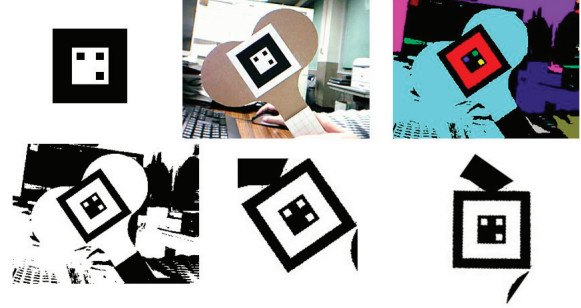


Figure 6: Marker recognition process example

4. Compare the registered pattern and the regularized rectangles to recognize the marker.

The implementation of AR toolkit has a similar process for detecting and recognizing registered binary markers [4]. We use some of the library codes in the AR toolkit for low-level image processing whose outputs correspond to the points pairs which are used for further triangulation by the stereo camera in our system.

6 BRAIN APPEARANCE MODEL

To help navigate the doctor in handling the coil to target the specific spot, we must describe the live spatial relation of the coil and the patient's brain. We prepared a 3D model of the brain on which the current coil position is mapped on for navigation display. We used software MRICro [13] to convert the MRI data in DICOM format to a set of intersectional images of a bitmap format. The easiest way to show the 3D brain is volume rendering with a colored point cloud, directly using the pixels of the bitmap intersections. However, the interest region for rTMS is the surface with a folded or wrinkled pattern, which shows brain mapping to locate the stimulation spot, depending on the pain region, for example. Volume rendering is not suitable for our visual context, because internal information not only is unnecessary, but also interferes with surface pattern visibility. Therefore, we create a polygon model of the surface shape with proper texture of the wrinkled pattern of the brain.

6.1 Texture Extraction

First, we manually extract the brain region in each intersection image, excluding the region of skin, bones, spinal fluid and etc. Secondly, Setting a polar coordinate with its origin at the center of the brain, the Cartesian coordinate (x, y, z) of every point from the intersectional image pixels can be mapped onto 2-dimensional angular space $\phi - \theta$, according to the following equations;

$$r = \sqrt{x^2 + y^2 + z^2} \quad (6)$$

$$\phi = \cos^{-1} \frac{y}{\sqrt{x^2 + y^2 + z^2}} \quad (7)$$

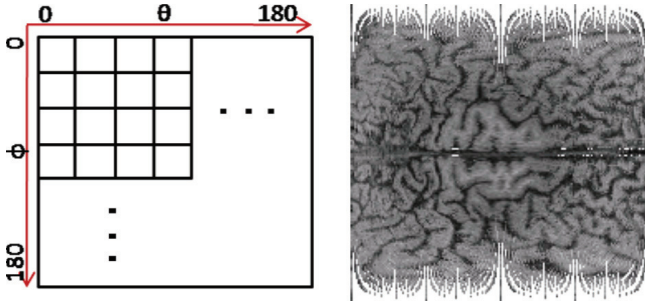


Figure 7: Brain Texture and its Coordinate

$$\theta = \cos^{-1} \frac{x}{\sqrt{x^2 + z^2}}, \quad (8)$$

where, the parameter r is the distance from the origin. The point with the largest r is the most distant from the center, namely the most nearest from the brain surface among the points in the same orientation bin of (ϕ, θ) . Finally, a 2-dimensional 180×180 array is prepared to contain the color of the point which is the nearest from surface at the (ϕ, θ) . This array can be used for the surface color pattern texture as shown in Figure 7(right).

6.2 Surface Mesh

To generate a surface of the brain, we utilize the contours of the original intersectional images in the MRI data. A rough approximation of the each contour with a polygon is used, and the vertices can be mapped onto the $\phi - \theta$ plane and re-sampled to be contained in another 2-dimensional 180×180 array as shown in Figure 8(left). Using 2-dimensional Delaunay triangulation, a triangle mesh network can be generated (8(middle)). In this network drawing the triangle mesh with the original 3D coordinate creates the surface shape of the brain. The $\phi - \theta$ map can be used as the texture coordinate and a surface shape is rendered with the corresponding texture as shown in Figure 8(right).

A navigation display can be prepared as shown in Figure 9, integrating the brain model, the coil position and orientation.

7 EXPERIMENTS

7.1 Implementation

We implemented the proposed method for constructing a prototype system, using the devices and software listed in Table 1. The stereo camera was assembled with two cameras that have an IEEE1394 bus connection. For the stereo matching process, we applied hardware programming with CUDA, GPU (graphical processing unit) architecture for parallel processing using software utilities by NVIDIA[11]. In this implementation, the highest computation cost in searching for correspondence between a stereo image pair is assigned to the CUDA processing with C-based coding.

We used 64 threads to compute the sum of squared differences (SSD) for every 11×11 block-size window in the left camera im-

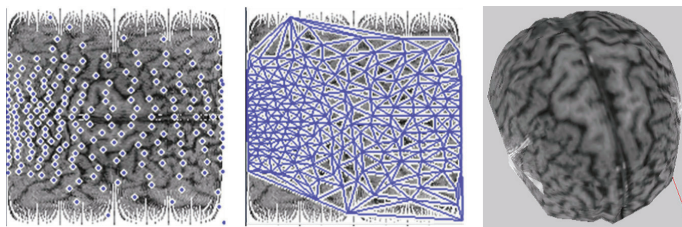


Figure 8: Brain Surface Model

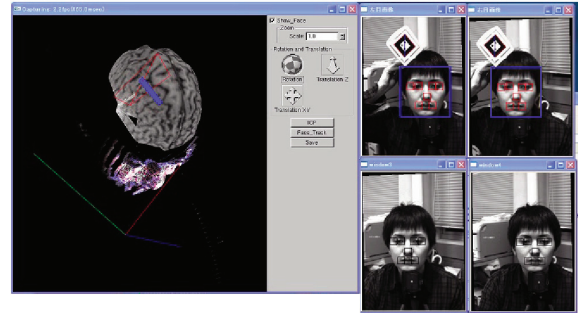


Figure 9: Navigation Display: The blue line shows the current coil position and orientation(left) and the marker detection and the face tracking are processed from the same image pair in parallel(right)

Table 1: Devices and Softwares for Prototyping

DLP Projector	TAXAN U6-232, Kaga Component Inc. 2500 lm 1024 x 768 pix
Camera	Dragonfly Express, Point Grey Research Inc. 640 x 480 pix
PC	CPU: Core2 Quad 2.66 GHz 3.0 GB RAM
Video Card	Quadro FX1700, Nvidia Inc.
Library	MS Visual studio on windows XP CUDA, OpenCV, OpenGL, ARToolkit, VTK[6]

age to search the corresponding area in right-camera image. The single thread computes the SSD for one column and the SSD of the both sides of the column are summed up to get a total block SSD and search the minimum SSD position effectively.

To capture the dense point cloud of the face shape for the initial alignment, we prepared a projector just behind the stereo camera to project a random dot pattern, which is created by dividing the VGA screen into 16×12 of $64 \text{ pixel} \times 64 \text{ pixel}$ blocks. We randomly put a 2×2 pixel size dot within each block.

7.2 Positioning Experiments

To clarify the result of the initial alignment, intersections are set up as shown in Figure 11. The red lines show the point clouds recorded by the stereo camera. The maximum residual displacement between the MRI surface and the point cloud from the stereo camera was 6.0 mm (Figure 11).

Using a human-like head model and a protractor (Figure 12), we investigated the tracking error. As shown in Figure 10, by assuming that the display monitor faces right in front of the patient and the stereo camera looks down the patient's face, the camera and the projector are set up. While the head model is rotated for every 2.5 degrees within ± 12.5 degrees range, the estimated tracked position by the proposed system and the directly measured positions were compared (Figure 13). For the tracking coil, the average error was 1.1 degrees rotation around each axis and 5.0 mm translation along each axis. Considering the target spot size is about 10 mm in diameter[3], achieved performance is feasible, but may require interactive trial-and-error to reach the proper spot.

8 CONCLUSION

This paper proposed a navigation system for visualizing the rTMS target by virtually superimposing MRI volume data onto a live patient's head position, using image measurement for 3D tracking in realtime. The combination of markerless tracking for the patient's

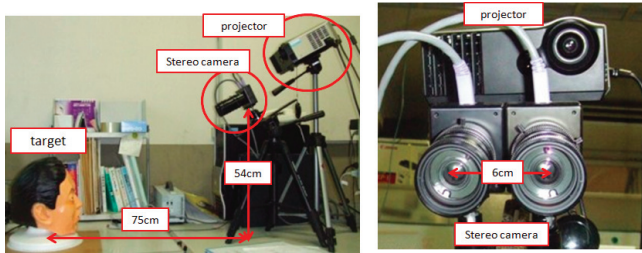


Figure 10: Stereo Camera Setup

head and marker tracking for the coil by an identical stereo camera showed good potential and feasibility for constraints-free rTMS treatment.

Our next step includes improving the stereo camera precision by an intensive sub-pixel process for disparity computation with a limited base-line length. Developing a user-friendly graphical user interface for not only specialized doctors but also generic doctors and patients themselves is also within our focus.

ACKNOWLEDGEMENTS

This work was supported in part by a grant from Teijin Pharma Limited.

REFERENCES

- [1] P. Besl and N. McKay. A method for registration of 3-d shapes. *IEEE Transactions on Pattern Analysis and Machine Intelligence*, 14:239–256, 1992.
- [2] T. Fukushima, A. Nishikawa, F. Miyazaki, K. Uchida, M. Sekino, and Y. Saitoh. Magnetic guided transcranial magnetic stimulation: Newly convenient navigation system. In *the 24th International Congress and Exhibition on Computer Assisted Radiology and Surgery (CARS2010)*, volume 5(supplement 1), pages S36–S37, June 2010.
- [3] A. Hirayama, Y. Saitoh, K. H. T. Shimokawa, S. Oshino, M. Hirata, A. Kato, and T. Yoshimine. Reduction of intractable deafferentation pain by navigation-guided repetitive transcranial magnetic stimulation of the primary motor cortex. In *Pain*, volume 122, pages 22–27, 1-2 2006.
- [4] H. Kato and M. Billinghurst. Marker tracking and hmd calibration for a video-based augmented reality conferencing system. In *Proceedings of the 2nd IEEE and ACM International Workshop on Augmented Reality*, pages 85–95, Washington, DC, USA, 1999. IEEE Computer Society.
- [5] G. Kindlmann. Semi-automatic generation of transfer functions for direct volume rendering. Master’s thesis, Cornell University, 1999.
- [6] Kitware, Inc. *The Visualization Toolkit User’s Guide*, January 2003.
- [7] R. Lienhart and J. Maydt. An extended set of haar-like features for rapid object detection. In *IEEE ICIP 2002*, pages 900–903, 2002.
- [8] The Magstim, Inc. *Magstim* <http://www.magstim.com/>.

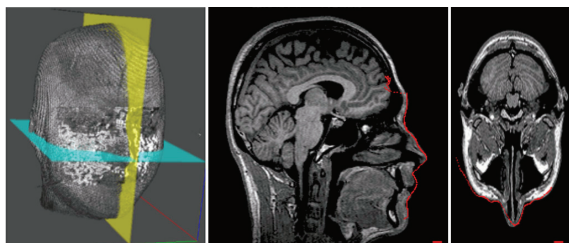


Figure 11: Initial Alignment Result: Red lines show the point cloud by the stereo camera.

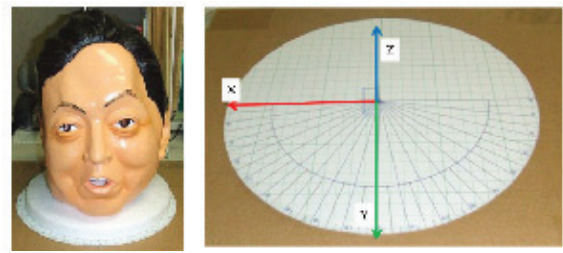


Figure 12: Experimental target

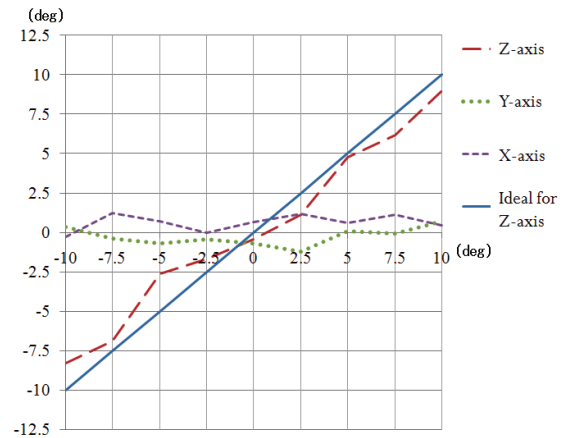


Figure 13: Tracking Error for Rotational Movement

- [9] Y. Matsumoto, J. Heinzmann, and A. Zelinsky. The essential components of human-friendly robot systems. In *Int. Conference on Field and Service Robotics*, pages 43–51, 1999.
- [10] NDI, Inc. *POLARIS*, <http://www.ndigital.com/medical/polarisfamily.php/>.
- [11] Nvidia, Inc. *CUDA* <http://developer.nvidia.com/category/zone/cuda-zone/x>.
- [12] T. Paus. Imaging the brain before, during, and after transcranial magnetic stimulation. *Neuropsychologia*, 37,2:219–224, 2001.
- [13] Principal Investigator; Neuropsychology Lab, Atlanta GA, USA. *MRIcro* <http://www.cabiatl.com/mricro/>.
- [14] P. Viola and M. Jones. Rapid object detection using a boosted cascade of simple features. *Computer Vision and Pattern Recognition, IEEE Computer Society Conference on*, 1:511, 2001.
- [15] Willowgarage. *OpenCV*; <http://opencv.willowgarage.com/>.